Modelling the role of cytotoxic T lymphocytes in tumour regression

Beck, R.J.

Chapter 3

Contact-Dependent Killing by Cytotoxic T Lymphocytes Is Insufficient for EL4 Tumor Regression in vivo

Richard J. Beck, Maarten Slagter and Joost B. Beltman

Division of Drug Discovery and Safety, Leiden Academic centre for Drug Research, Leiden University, Leiden, The Netherlands

Cancer research 79.13 (2019): 3406-3416.

Abstract

Immunotherapies are an emerging strategy for treatment of solid tumors. Improved understanding of the mechanisms employed by cytotoxic T lymphocytes (CTLs) to control tumors will aid in the development of immunotherapies. CTLs can directly kill tumor cells in a contact-dependent manner or may exert indirect effects on tumor cells via secretion of cytokines. Here we aim to quantify the importance of these mechanisms in murine thymoma EL4/EG7 cells. We developed an agent-based model (ABM) and an ordinary differential equation (ODE) model of tumor regression after adoptive transfer of a population of CTLs. Models were parameterized based on in vivo measurements of CTL infiltration and killing rates applied to EL4/EG7 tumors and OTI T cells. We quantified whether infiltrating CTLs are capable of controlling tumors through only direct, contact-dependent killing. Both models agreed that the low measured killing rate of CTLs in vivo was insufficient to cause tumor regression. In our ABM we also simulated CTL production of the cytokine interferon gamma (IFNγ) in order to explore how an antiproliferative effect of IFNγ might aid CTLs in tumor control. In this model IFNγ substantially reduced tumor growth compared to direct killing alone. Collectively these data demonstrate that contact-dependent killing is insufficient for EL4 regression in vivo and highlight the potential importance of cytokine-induced antiproliferative effects in T cell mediated tumor control.

Introduction

In the last decade, immunotherapies for cancer have moved into the mainstream of clinical oncology. Antibodies targeting immune checkpoints have been particularly successful, offering significant advantages over chemotherapy in a range of advanced metastatic, relapsed, and refractory solid tumors. CTLA-4, PD-1, and PD-L1 inhibitors are now approved in melanoma, non-small-cell lung cancer, renal cell carcinoma, urothelial carcinoma, merkel cell carcinoma, and some colon cancers[1]. Another promising immunotherapeutic approach has been the transfer of large numbers of cytotoxic T lymphocytes (CTLs). The transferred cells can be either autologously derived tumor infiltrating lymphocytes (TILs), or engineered with a chimeric antigen receptor (CAR) for tumor specificity. 2017 saw the first FDA approvals of CAR T cells for treatment of B cell malignancies[2]. The potential of adoptive transfer therapies for solid tumors has been highlighted in trials using TILs against melanoma[3–5], or CAR T cells against a range of solid tumors[6–8]. However, these promising early results have so far failed to transfer into the clinic.

Many attempts are being made to improve the efficacy and broaden the scope of cancer immunotherapies. For example, immunotherapies can have a synergistic effect when applied together with other immunotherapies[9,10], or with traditional treatments such as radiotherapy and chemotherapy[11,12]. Optimal treatment scheduling and dosages are yet to be determined. Given the danger of life threatening immune related adverse events following immunotherapy as well as the high costs involved, biomarkers to indicate which patients are likely to benefit from these treatments will be highly valuable. In particular, the immunosuppressive microenvironment which often characterises solid tumors represents a significant hurdle to the expansion and improvement of immunotherapies. Given the complex nature of the various mechanisms of interaction involved in determining the success of immunotherapies, a quantitative understanding of the contribution of these various mechanisms will be highly beneficial for the rational design and optimisation of cancer immunotherapies.

One highly relevant topic requiring greater quantitative insight regards the mechanisms employed by CTLs to control tumors *in vivo*. Indeed, these cells are key players in anti-tumor immune responses, which they are thought to achieve through being extremely efficient killers. This reputation has primarily been established by *in vitro* studies showing evidence of serial or simultaneous killing of several target cells in a short time frame[13,14]. Killing by CTLs is usually considered to be ‘direct’, i.e., contact dependent, and mediated by either perforin and granzymes, or FAS-L. Several studies have suggested that direct lysis of tumor cells by CTLs is extremely important in tumor control[15–18]. However, the reported killing rates of CTLs *in vivo* are typically low[19] and it is not clear whether these rates are indeed sufficient for control of tumors. Several studies have highlighted the importance of ‘indirect’ effects of cytokine signalling by activated T cells in the control of tumors, in particular IFNγ [20,21]. IFNγ may control tumors by exertion of an antiproliferative effect[22], sensitization of tumor cells to FAS-L mediated death[23], recruitment of effector cells of the innate immune system[24], and by causing widespread necrosis of tumor cells along with tumor vasculature destruction[25].

In the current study we quantitatively compare the importance of direct, contact dependent killing, with indirect cytokine mediated tumor control, based on published experiments in which EL4/EG7 tumor cells were infused into mice[18]. We chose to focus on the EL4 tumor cell line which, along with its transformed Ova antigen expressing derivative EG7, has been widely used to explore the anti-tumor activities of CTLs in an *in vivo* setting[18,21,26–29]. Using these cell lines, evidence has emerged supporting an important role for IFNγ in tumor control by CTLs yet a negligible role for direct killing, along with apparently contradictory evidence suggesting an important role for direct killing. Hollenbaugh *et al.[30]* transferred perforin and FasL deficient T cells into EG7 tumor bearing mice, and these deficient T cells were able to control tumors almost as well as their wild type counterparts. However, IFNγ deficient T cells displayed a marked reduction in tumor control, suggesting that IFNγ rather than direct cytotoxicity was the primary mechanism used by CTLs to control the tumor. In contrast, Breart *et al.[18]* used intravital two-photon imaging to show that apoptotic events almost exclusively occurred when tumor cells were contacted by T cells, thus arguing for a major role of direct cytotoxicity. Moreover, they generated mixed tumors, comprising both Ova-expressing EG7 cells and non-Ova-expressing EL4 cells. In these mixed tumors only the antigen expressing EG7 cells were eliminated, arguing against an indiscriminate effect from IFNγ. We integrate the data acquired at various levels into both an ordinary differential equation (ODE) model, and a spatial agent-based model (ABM). Applying these models to the *in vivo* data we show that the observed T cell densities and slow killing rate were insufficient to explain the population-level tumor regression observed in the mice. We found that an antiproliferative effect mediated through IFNγ signalling allowed CTLs to influence far more cells than direct killing alone, therefore leading to a substantially greater impact on tumor progression. Our modelled scenario corroborated the notion that IFNγ plays a crucial role in EL4 tumor control, and reconciles this with the apparently conflicting observation of low reported killing rates and density of infiltrating CTLs.

Methods

Data interpretation

Since the main aim of this work is to test whether CTLs could have controlled the tumor through the sole means of direct killing, we favoured ‘optimism’ from the CTL viewpoint wherever the *in vivo* dataset was ambiguous. Thus, we chose model assumptions that promoted tumor control through direct CTL killing.

Tumor Cells. Tumor volume measurements in the absence of CTL transfer were used to fit the growth rate of both our ODE model and ABM. Based on manual counting of the images, we estimated that the density of tumor cells was approximately 10^6 cells mm^{-3}. This value is the default used in all our models. Moreover, Breart *et al.[18]* used flow cytometry to estimate the absolute number of tumor cells inside two tumors 10 days after inception (in the absence of infused T cells). An average of 4×10^6 cells were recovered, at a time-point where the average tumor volume was ~$17mm^3$, corresponding to a density of approximately 0.25×10^6 cells mm^{-3}. Given that a substantial fraction of tumor cells were likely lost during the cell isolation procedure[31], this can be viewed as an absolute underestimate of the tumor cell density. To

convert between tumor volume and number of tumor cells, we consider direct proportionality between these quantities.

Dead tumor cells are not recognised by CTLs in our models yet are not immediately removed from the models. Parnaik *et al. [32]* found that cultured rat cerebellar neurons were completely cleared within 3 hours of apoptosis by professionally phagocytic microglia, whereas the same cells were incompletely cleared after 9 hours by non-professionally phagocytic epithelial cells. We therefore considered tumor cells to persist for an average of 6 hours after apoptosis. Because the number of CTLs in our modelled tumors is proportional to the tumor volume (the sum of numbers of dead and alive cells), inclusion of dead tumor cells increases the ratio of effector : alive target (E:T ratio) and thereby increases the total killing rate.

CTLs. Breart *et al.[18]* transferred CTLs to mice on day 5 after tumor injection. Before this point we consider CTLs to be absent from the tumor. Because killing undertaken by any endogenous CTL should also occur in the control tumors where no CTLs were transferred, this is already accounted for in our fit to the tumor growth data in the absence of CTLs. Breart *et al.[18]* measured the density of CTLs within the tumor on days 7 (12500 CTLs mm^{-3}) and 8 (25000 CTLs mm^{-3}). Based on our estimate of 10^6 tumor cells mm^{-3}, this corresponds to an Effector:Target ratio of 1:80 on day 7, and 1:40 on day 8. Due to the temporally sparse measurements the exact dynamics of T cell infiltration into the tumor are not known and for simplicity we linearly interpolated between the available data points. Beyond day 8, further data on the density of infiltrating CTLs was not recorded. In reality T cell numbers likely peak and then decline a few days after adoptive transfer[22], and T cells often suffer from exhaustion after extended time in the tumor[33,34]. However, it is certainly possible that CTL numbers continued to increase beyond day 8. In line with our policy of taking the most optimistic assumptions from the CTL viewpoint, we considered the ratio of effector T cells to total tumor cells (Effector:Tumor-Cell ratio) to continue to linearly increase after day 8. Also in line with our policy, we do not consider CTLs to diminish in effector function over time (which would make it more difficult to control the tumor). CTLs kill tumor cells at a default rate of $k = 4\ CTL^{-1}\ day^{-1}$.

ODE Model

Model setup. ODE simulations were performed in the R language, using the package 'deSolve 1.14'. Models were fitted using the Levenberg Marquardt algorithm in the package 'minpack.lm 1.2-1'. Our ODE model was designed to test whether CTLs could control tumors with the observed direct killing rate of $k = 4$ kills $CTL^{-1}\ day^{-1}$. Therefore, we deliberately simplified the model, with assumptions chosen to maximise the likelihood of tumor control. The model consists of two coupled equations:

$$\frac{dT}{dt} = gT - kE(t)\ , \qquad (1)$$

$$\frac{dD}{dt} = kE(t) - dD, \tag{2}$$

Thus, tumor cells *T* are considered to grow exponentially with rate *g (day^{-1})* in the absence of CTLs, because the experimental tumors clearly did not yet suffer from competition for resources during the measurement interval (Fig. 1A). Tumor cells are killed at rate *k (CTL^{-1} day^{-1})* by a population of effector cells *E(t)*, where E(t) is determined based on the number of dead and alive tumor cells (Data Interpretation, Fig. 1B):

$$\mathrm{E}(t) = \lambda(T + D)\begin{cases} 0 & if\ (t \leq 5) \\ (t-5) & if\ (5 < t \leq 7) \\ 2\big(1 + (t-7)\big) & if\ (7 < t), \end{cases} \tag{3}$$

with the parameter λ arising from interpolation of the data ($\lambda = \frac{1}{160} cell^{-1}\ day^{-1}$), which defines the rate of increase in the Effector:Tumor-Cell ratio $E:(T + D)$.

Killed cells *D* are cleared at rate *d (day^{-1})*. We took the killing rate to be proportional to the number of CTLs and independent of the number of target cells, implying that CTLs are considered to always kill at their maximal rate. In reality a dual saturation function, with saturation in both effector and tumor cell number T, is a more complete description of CTL killing (Supplementary Methods) [35,36]. However, we aimed to model a situation that favours CTL control of the tumor. In such a best-case scenario from the CTL viewpoint, CTLs always have sufficient targets to kill and need never search for targets. As such our simplified ODE model is an extremely optimistic scenario from the point of view of the CTLs. This simplification implies that our model is a good approximation as long as the E:T ratio remains sufficiently low.

ABM

Model setup. ABM simulations were implemented in C++14, using boost 1.69.0. Visualisations were rendered in C++ using VTK 8.0. We use an asynchronously updating ABM to simulate tumor growth, T cell infiltration and migration, and tumor regression. Our ABM features two types of agents: CTLs and tumor cells. Tumor cells live on a regular 3D lattice where each cell occupies a single lattice site; tumor cells do not share sites with each other. Empty sites in the lattice represent extracellular matrix, or other cell types not interfering with the tumor. Lattice sites have length 10μm by default, roughly corresponding to our default tumor cell density assumptions. Each tumor cell grid point contains information on the tumor cell type (either EG7 or EL4), the amount of damage it has sustained from CTL attacks, and whether it is alive or not. Throughout the simulation we track the displacement of the furthest tumor cell from the centre of the lattice; this measurement is used to dynamically adjust the size of the simulation domain. The domain is a sphere, extending from the lattice centre out to a radius 5 lattice sites (50μm) beyond the displacement of the furthest tumor cell.

Tumor cell behaviour. The tumor is initialised on day 0, by filling *T0* lattice sites with tumor cells within a radius o*f* R_i from the lattice centre. The simulation is advanced in timesteps of 1 minute *(Δt)*. At each timestep each tumor cell is liable to to replicate with probability *gΔt*. Cells replicate into a random neighbouring square if one is available. We implemented short range dispersal (similar to [37]) as a computationally inexpensive means to achieve exponential, spheroidal tumor growth whilst comfortably allowing simulation of over 10^8 individual agents. Candidate dividing cells whose surroundings are fully occupied attempt to disperse from the tumor with probability p_{disp}. Dispersing cells produce a daughter cell for which a new location is chosen based on a random walk with mean dispersal distance proportional to the current tumor radius. If the chosen site is vacant the daughter cell occupies this site, otherwise the dispersal attempt fails.

CTL infiltration. CTLs are associated with a location corresponding to a grid site, however they are not explicitly represented on the grid and as such can share space with other CTLs or tumor cells. Thus, CTLs do not contribute to the tumor mass and are able to move through tumor tissue, attempting to form conjugates with antigen expressing tumor cells. We allowed for such co-occupancy because CTLs can easily move in between other cells in densely packed environments such as a lymph node[38] or the skin epidermis[39], and are able to cooperate to kill individual targets[19]. Because of the relatively low Effector:Tumor-Cell ratios observed in the experimental data, in practise our CTLs rarely share lattice sites. Specifically, two or more CTLs share a lattice site only ~2% of the time, and 3 or more share a site ~0.01% of the time on day 8 of a typical simulation. Following the experimental setup, CTLs infiltrate the tumor on day 5 after tumor inception. New CTLs arrive at random points within the existing simulation domain. At each timestep a target number of CTLs is calculated based on the Effector:Tumor-Cell ratio we estimated from the data (in equivalence with the ODE model). If the number of CTLs inside the simulation is below the current target, new CTLs are added to the simulation until the target is reached. CTLs are only removed from the simulation when they migrate outside the simulation domain. The number of CTLs may therefore exceed the target density, albeit only whilst the tumor disappears more quickly than CTLs migrate out of the simulation domain.

CTL migration. CTLs migrate until they reach a site occupied by a tumor cell; CTLs that migrate outside the simulation domain are removed. Whilst a CTL is migrating, each time-step it randomly moves to an adjacent lattice site within its 3D Moore neighbourhood including its current location. Thus, there is a 1/27 probability of no movement, a 6/27 probability of a 10 μm movement, 8/27 probability of a$10\sqrt{2}$μm movement, and a 8/27 probability of a $10\sqrt{3}$μm movement. Therefore, the resulting migration speed is 11.5μm per minute, which is in close agreement with previously measured values in the EL4/EG7 tumor [29]. CTLs that find tumor cells arrest with probability p_{arr}, and subsequently attack tumor cells with probability p_{hit} or detach and resume migration with probability p_{det}. By default $p_{arr} = 1$ and $p_{det} = 0$, although these are varied to $p_{arr} = 0.9$ and $p_{det} = 0.01$ in the simulations where we examine multi hitting CTL. CTLs are immediately released from conjugates if the target cell dies.

Effects of CTLs on tumor cells. Tumor cells may sustain n_{hit} hits from CTLS before apoptosis occurs. By default $n_{hit} = 1$, in which case CTLs attack targets with an attack rate identical to the killing rate. In simulations where multiple hits are required for tumor cell death the base attack rate is multiplied by the number of hits required for apoptosis. Therefore the overall killing potential

of the CTLs is controlled between single-hit and multiple-hit simulations to obtain equal killing rates.

In simulations with IFNγ, that cytokine is produced at a constant rate by CTLs whilst conjugated with tumor cells. IFNγ is consumed by tumor cells, and tumor cells cannot divide when the local IFNγ concentration exceeds a threshold value. We set the diffusion parameters such that the threshold occurs at around 3 cell lengths away from a conjugated CTL. For details see the Supplementary Methods.

Mixed tumors. We simulated mixed EL4/EG7 tumors by seeding a 50/50 mixture of cells on day 0. The only difference between these cell types is that EG7 cells are not recognised by CTLs.

Results

Direct CTL cytotoxicity is not sufficient to mediate *in vivo* regression of EG7 tumors

In the *in vivo* data of Breart *et al.[18]*, transferred OTI effector T cells rapidly controlled an infused EG7 tumor, following direct contact with tumor cells. However, each infiltrating CTL killed on average only 4 tumor cells per day and it is unclear if tumor regression should be expected based on the density and cytotoxic activity observed in this *in vivo* data. To test whether CTLs could reasonably be expected to control the *in vivo* tumors, we employed an ODE model (see Methods) that integrated the measurements made at various levels. Instead of providing a detailed description of the tumor and its interactions with the immune system, the goal of this model was rather to assess the possibility that direct killing could have solely accounted for tumor regression. The simplifications that we made in the ODE model always favoured the CTLs, i.e., they made tumor regression more likely. If indeed CTLs were capable of controlling the tumor by direct killing alone, tumor regression would certainly be observed in this simplified model.

Modelling tumor growth as an exponential process resulted in a good match to the tumor measurements from Breart *et al.[18]* for the case without T cell transfer (Fig. 1A), suggesting that tumor growth was not yet inhibited by factors such as competition for nutrients. Subsequently, we introduced a population of CTLs into this model, with Effector:Tumor-Cell ratio based also upon experimental measurements (Fig. 1B). The impact on the tumor was limited when CTLs killed tumor cells at a rate of $k=4\ CTL^{-1}day^{-1}$ as reported by Breart *et al.[18]* (Fig. 1C), despite the continuous increase in intratumoral T cell numbers (Fig. 1D). The killing rate measurements were relatively uncertain compared to the other parameters in the ODE model, perhaps having varied over time or throughout the tumor. To address that uncertainty,we simulated CTL populations killing with rate up to $k=16\ CTL^{-1}day^{-1}$, which is at the high end of the range of reported estimates for CTL killing performance *in vivo* [40]. As a side note, in this model such a 4-fold increase of the killing rate is equivalent to a 4-fold increase of the CTL infiltration rate. With $k=16$ our simulated tumors were controlled, although this control occurred only at much later time points than was the case for the *in vivo* tumors. Thus, even for the extremely optimistic scenario we consider and using a substantially higher killing rate than was measured experimentally, direct CTL lysis alone could not explain the observed *in vivo* tumor regression.

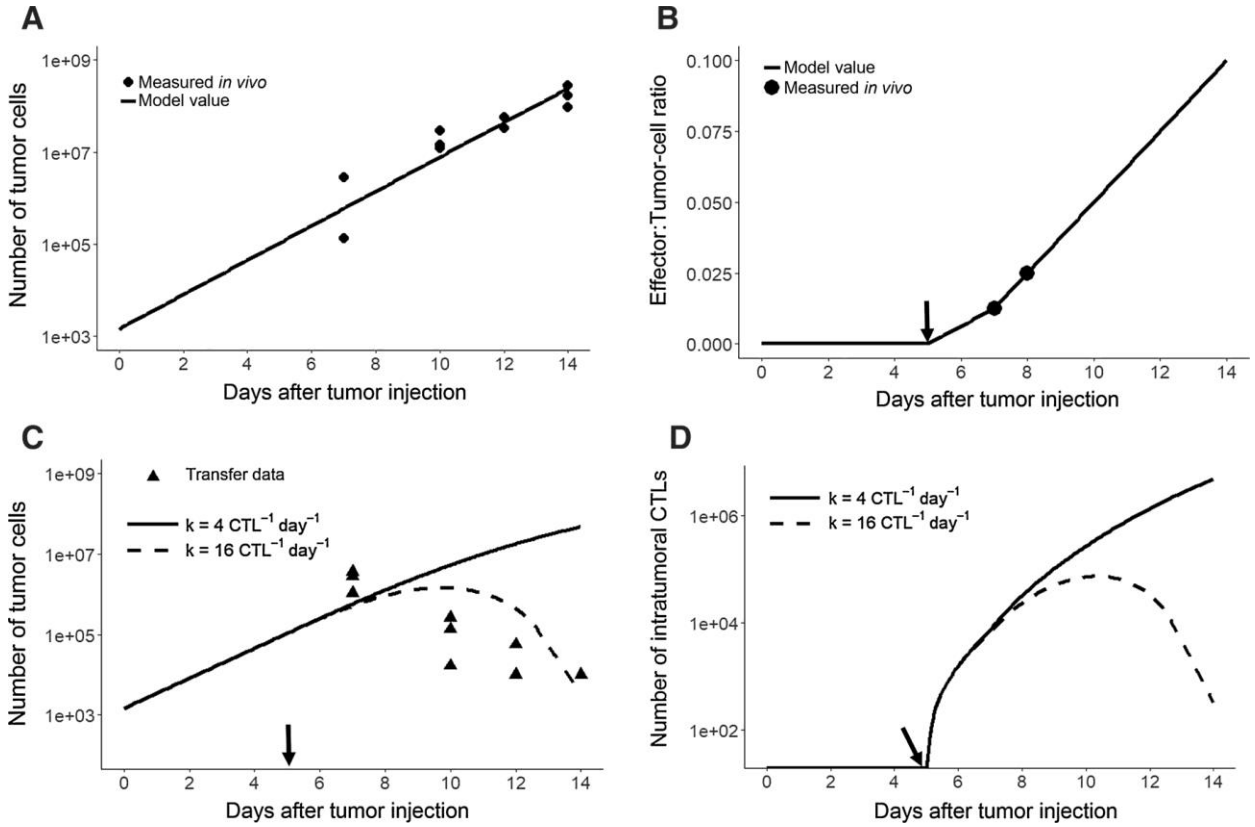

Figure 1. ODE model suggests direct T cell cytotoxicity is insufficient for control of EG7 tumors. **A)** Tumor growth is described as exponential growth (g=0.86 day^{-1}). **B)** Effector:Tumor-Cell ratio in the ODE model is estimated by linear interpolation of measured data points. After day 8, we assume a linear increase in CTL density. Arrows in **B-D** indicate time of CTL transfer. **C)** ODE simulation of tumor dynamics in the presence of actively killing CTLs, with two different killing rates. Lines represent model fits and dots represent experimental data. **D)** Total number of CTLs in simulations with killing.

Agent Based Model supports notion that CTL cytotoxicity is insufficient to mediate *in vivo* regression of EG7 tumors

We developed a spatially explicit ABM with tumor cells and CTLs as agents to contrast against the idealised ODE model (Fig. 2A-B). As in the ODE model, in the ABM the overall growth rate of the tumor was matched to the data in the absence of CTLs (Fig. 2C), although the ABM differs in that tumor cells cannot divide when fully surrounded, i.e., there is competition for space. Tumors were much less well controlled in the ABM than they were in the ODE model (Fig. 2D); even at a killing rate of $k=16\ CTL^{-1}day^{-1}$ the tumor was not controlled in the ABM. There are two reasons for this discrepancy. Firstly, when compared to the ODE model, the ABM has the added requirement that CTLs must migrate in order to find tumor cells to kill. Indeed, the fraction of CTLs in conjugates was lower in simulations with $k=16\ CTL^{-1}day^{-1}$ than in those with $k=4\ CTL^{-1}day^{-1}$(Fig. 2E), because faster killing CTLs spend less time conjugated with tumor cells. The second source of discrepancy between the ODE and ABM results stems from the competition for space between tumor cells that occurs in our ABM; CTL killing eases such competition, so tumor control is more difficult. Thus, the idealised ABM highlights that CTLs might make their own job more difficult by

being highly efficient killers. Overall, the ABM simulations confirm that CTL-mediated direct killing alone cannot explain EG7 tumor regression.

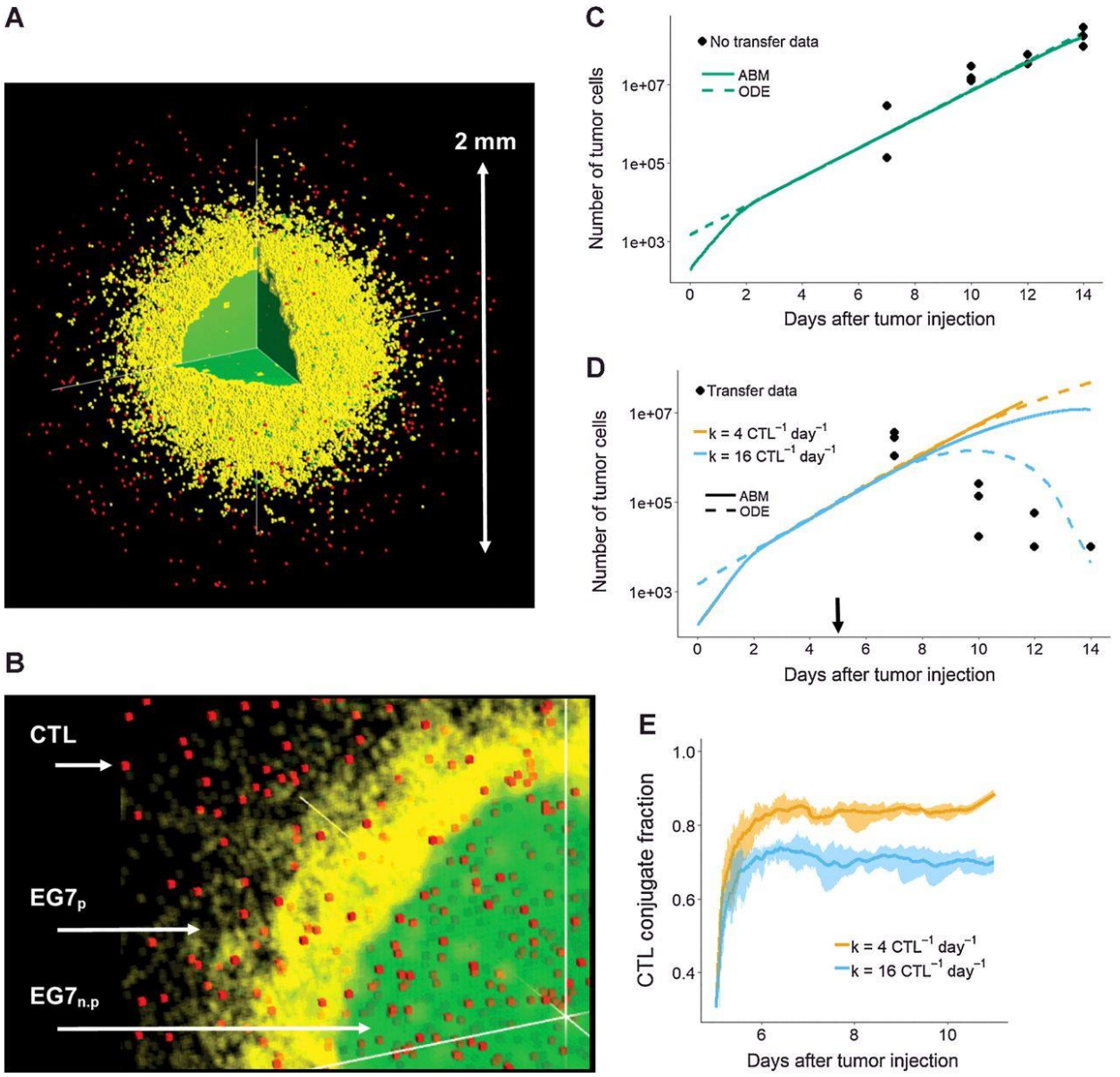

Figure 2. ABM confirms that direct T cell cytotoxicity is insufficient for control of EG7 tumors. **A-B)** ABM tumor infiltrated by CTLs on day 7. EG7 with free adjacent lattice sites can proliferate ($EG7_p$). EG7 with no free adjacent lattice sites are non-proliferating ($EG7_{n.p}$), although they may still disperse (see Methods). **C-D)** Comparison of tumor evolution in ABM (solid lines) and ODE model (dashed lines) without **(C)** and with **(D)** transferred CTLs, where arrow indicates time of CTL transfer. **E)** Fraction of CTLs in a conjugate with a tumor cell throughout ABM simulations.

IFNγ-mediated cell cycle arrest is sufficient for tumor control

Because IFNγ has been widely implicated in tumor eradication [20,21,23–25,41], we added production and diffusion of this cytokine to our ABM. We focussed on an antiproliferative effect of IFNγ because Breart *et al.[18]* only detected apoptosis in tumor cells directly contacted by CTLs, an observation which is inconsistent with the notion of significant IFNγ cytotoxicity towards EG7 cells. To test the contribution of the putative antiproliferative effect of IFNγ, we simulated tumors with $k=4\ CTL^{-1}day^{-1}$ or $k=16\ CTL^{-1}day^{-1}$, in the presence or absence of IFNγ. In our simulated tumors, the antiproliferative effect of IFNγ was much stronger than the contact dependent CTL lysis, even with $k=16\ CTL^{-1}day^{-1}$ (Fig. 3A). Although tumors were rapidly controlled in our model with IFNγ, they were not entirely eradicated. This can be explained by the low number of CTLs in the IFNγ simulations (Fig. 3B), together with the fraction of conjugated CTLs which drops after the onset of tumor regression for $k=16\ CTL^{-1}day^{-1}$ (Fig. 3C). CTLs mostly eradicate tumor cells in the centre of the spheroid, but some pockets of tumor cells in the periphery survive and allow the tumor to escape (Fig. 3D, Video S2). These modelled behaviours are consistent with literature observations that solid tumors "melt from the inside" [42], and that EL4 tumors may rebound after an initial response to transferred CTLs [43]. In summary, tumor cell cycle arrest due to cytokine production by CTLs in addition to their cytotoxicity can explain the observed response of EG7 cells to a population of transferred CTLs.

CTL cooperativity leads to heterogeneity in killing rate

Our ABM predicted an almost negligible role for direct killing in tumor regression, with or without the presence of IFNγ. However, the CTL killing rate may in reality have been higher than the measured $k=4\ CTL^{-1}day^{-1}$ and may not have been constant over time [36]. Factors that could play a role here include the ability of CTLs to kill collaboratively [19] and that of cancer cells to resist multiple CTL 'hits' before apoptosis is triggered [44]. We therefore used our ABM to assess whether the measurement of $k=4\ CTL^{-1}day^{-1}$ could have resulted from a higher 'intrinsic' CTL killing rate. We compared simulations in which tumor cells die after a single 'lethal hit' with simulations where an accumulation of several hits was required for apoptosis. There was no substantive difference between the single hit and multi hit scenarios in terms of tumor growth (Fig. 4A), or number of CTLs (Fig. 4B). At early time points, the fraction of CTLs in conjugates in the multi hit model was slightly higher than in the single hit model (Fig. 4C) and the temporal pattern of killing rate per simulated CTL (Fig. 4D) or per conjugated CTL (Fig. 4E) differs between the two settings. Multi hitting CTL populations initially killed at a low rate, because targets had generally not acquired enough damage to die. Subsequently, targets accumulated damage and the manifested killing rate per conjugated CTL rose above the killing rate for the single hit scenario (Fig. 4E). Similar to the killing rate-measurement procedure of Breart *et al.* [18], we measured killing in 100**μ**m x 100**μ**m x 30**μ**m 'windows' for a two hour period at the beginning of day 8 during a cumulative total of 75 hours of conjugated CTL imaging time[18]. Our analysis shows that such sample sizes in general reflect the global killing rate well (Fig. 4F). As a side note, in our model the infiltration of the tumors by CTLs was relatively homogeneous, meaning that damage to targets occurred roughly evenly throughout the tumor (Fig. 4G). Although heterogeneous infiltration may lead to strong spatial variability in killing rate, we conclude that temporal variation in killing is likely large, especially when CTLs cooperate.

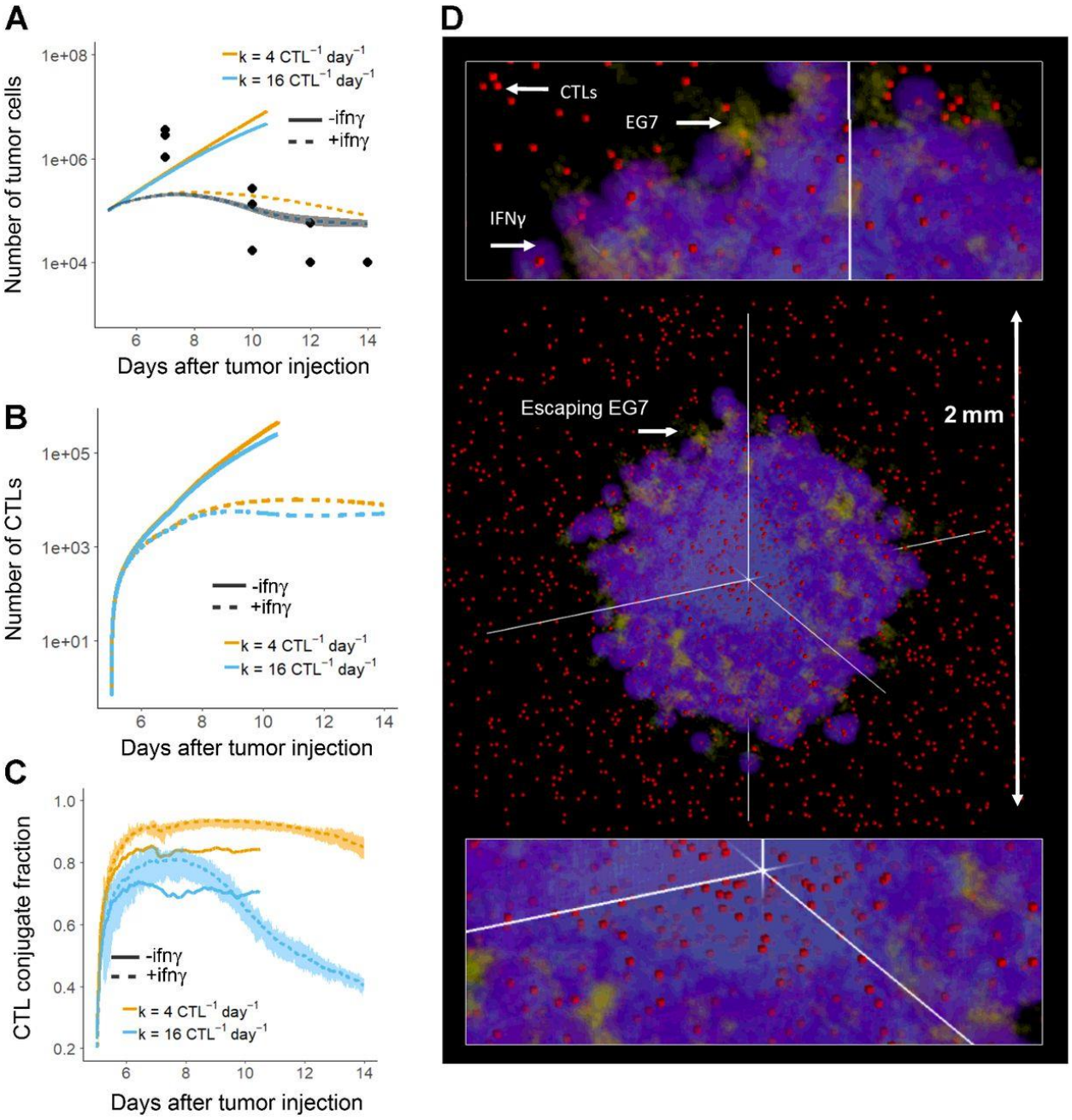

Figure 3. Antiproliferative IFNγ leads to tumor control. **A)** Simulated tumor volume compared with and without IFNγ producing CTLs. **B)** Total CTL numbers in simulations with or without IFNγ. **C)** Fraction of CTLs in conjugates in simulations with and without IFNγ. **D)** Tumor on day 8, in the presence of IFNγ.

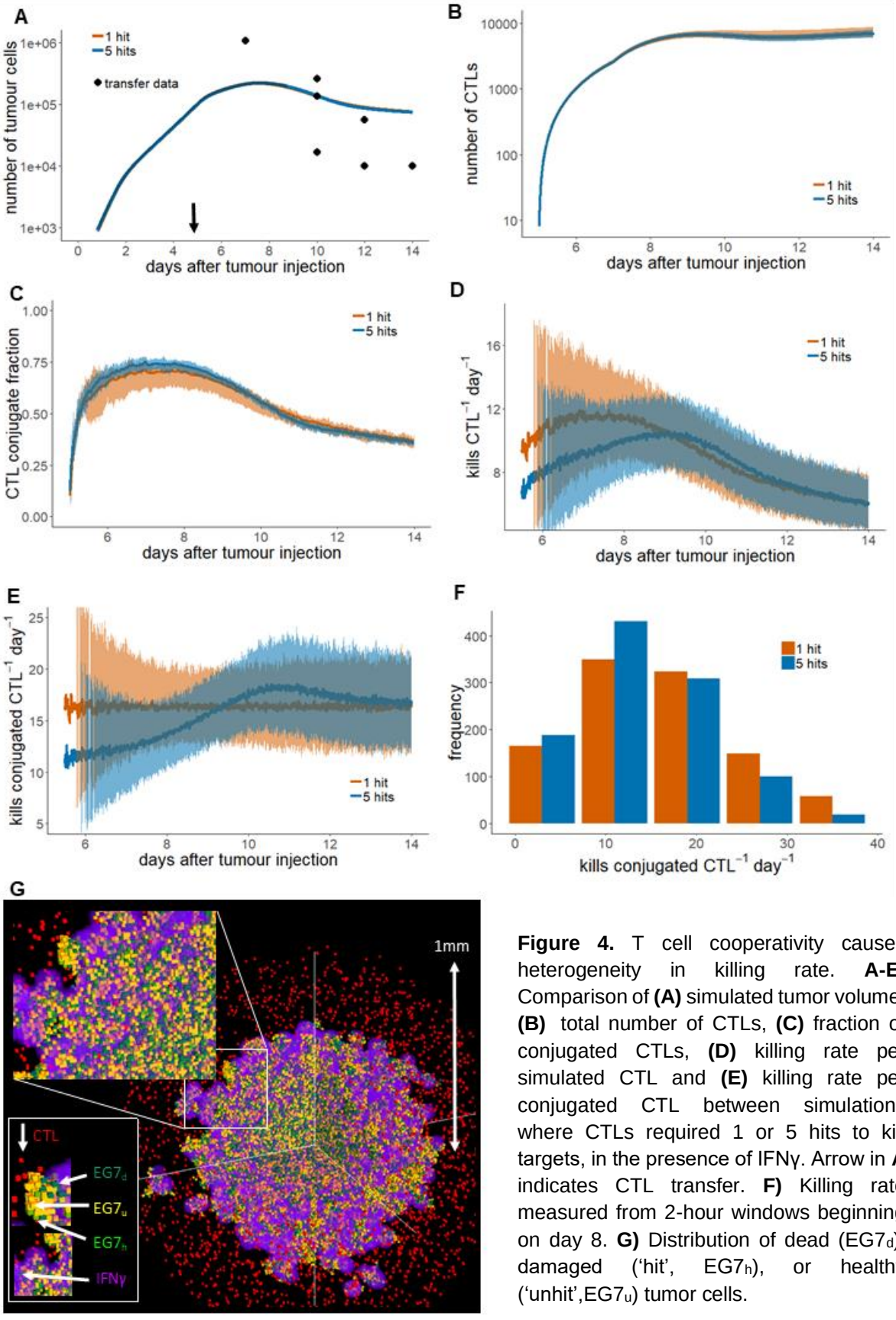

Figure 4. T cell cooperativity causes heterogeneity in killing rate. **A-E)** Comparison of **(A)** simulated tumor volume**,** **(B)** total number of CTLs, **(C)** fraction of conjugated CTLs, **(D)** killing rate per simulated CTL and **(E)** killing rate per conjugated CTL between simulations where CTLs required 1 or 5 hits to kill targets, in the presence of IFNγ. Arrow in **A** indicates CTL transfer. **F)** Killing rate measured from 2-hour windows beginning on day 8. **G)** Distribution of dead ($EG7_d$), damaged ('hit', $EG7_h$), or healthy ('unhit',$EG7_u$) tumor cells.

Direct killing plus antiproliferative IFNγ accounts for selective elimination of antigen positive cells

Breart *et al.[18]* noted that in mixed EL4/EG7 tumors, the non-cognate antigen expressing tumor cells (EL4) grew more or less unconstrained and it is unclear whether the antiproliferative effect of IFNγ is consistent with this finding. We therefore simulated mixed tumors, containing patches of antigen positive EG7 cells or antigen negative EL4 cells. EL4 cells were considered not to be recognized and thus not affected by direct interactions with CTLs, but could be affected by IFNγ that diffused from nearby locations. When initialised with a 50% mixture of EL4/EG7 cells, our simulated tumors form patches with similar spatial dimensions to the images from Breart *et. al.* (Fig. 5A). We simulated the transfer of CTLs into the mixed tumor model, upon which CTLs preferentially accumulated in regions of Ova-expressing EG7 cells where they began killing these cells and secreting IFNγ (Fig. 5B,Video S3). IFNγ concentrations were generally higher in regions of EG7 cells compared to regions of EL4 cells, yet despite the limited (~30 μm) range of IFNγ diffusion in our model many EL4 cells were prevented from replicating for a period of approximately 2 days, when the activity of the CTLs was greatest (Fig. 5C). By day 10 most EG7 cells were eliminated, and the CTLs, being deprived of stimulation, stopped producing IFNγ. After this point EL4 cells resumed growth, eventually filling the spaces left behind by the dead EG7 cells. EL4 cells were thus not so much affected by the presence of the CTLs. In conclusion, local production of anti-proliferative IFNγ is consistent with the experimental observation that within mixed tumors primarily cognate-antigen expressing cells were cleared by CTLs.

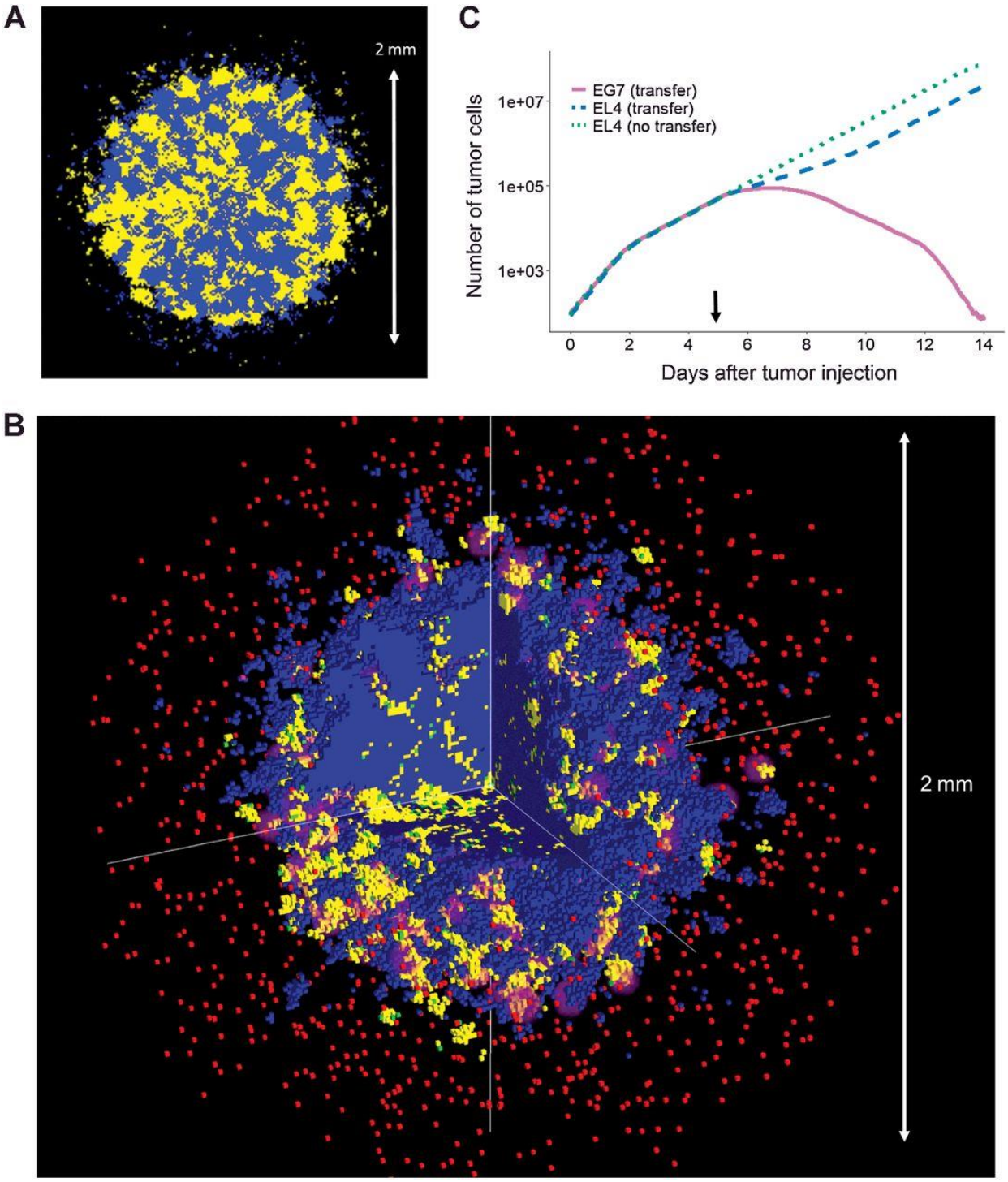

Figure 5. Antiproliferative IFNγ explains selective destruction of EG7 cells within EG7/EL4 mixed tumors. **A)** Example 2D slice from the centre of a simulated mixed tumor 8 days after tumor inception. **B)** Images showing examples of tumor composition (T cells in red, EG7 cells in yellow, EL4 cells in blue and IFNγ concentrations in purple) on day 8 during the course of EG7 regression. **C)** Evolution of the total volume of EG7 or EL4 cells in mixed tumor simulations. Arrow indicates time of CTL transfer.

Discussion

Immunotherapies involving CTLs are able to mediate regression or tumor control in cancers that were previously out of reach for conventional treatments. Despite major progress, many patients fail to respond, and the mechanistic insight required to explain this disparity in outcomes is lacking. Lysis of infected or malignant cells following direct physical contact is the canonical CTL effector function, but indirect effects of CTLs such as production of cytokines are increasingly recognised as having an important role in CTL mediated tumor regression[21,22,25,45]. The relative importance of these different mechanisms remains unclear and is likely to depend on characteristics of both the tumor and the T cells involved. Here we developed an ABM and an ODE model of tumor regression following adoptive transfer of a population of CTLs attacking EL4/EG7 tumor cells. Using these models, we attempted to quantify the relative contribution of direct CTL killing towards tumor regression in the EL4/EG7 model. Our simulated tumors were not controlled by direct CTL killing only, so we conclude that direct killing was not a sufficient explanation for regression in the EL4 tumor model.

In our ABM we also included simulation of an antiproliferative effect of IFNγ, because Hollenbaugh et. al.[21] observed that IFNγ deficient T cells display substantially reduced tumor controlling abilities. We modelled an antiproliferative effect because the tumor cells were only observed to die after CTL contact, evidence against a substantial long distance cytotoxic effect of IFNγ in this *in vivo* setting. IFNγ secreted by CTLs has been shown to contribute to regression in a different tumor model[22], by arresting the cell cycle of tumor cells. Although IFNγ has no direct antiproliferative effect on EL4 cells *in vitro[22]* it has been shown that nitric oxide (NO) is secreted by stromal cells after exposure to IFNγ[21]. Such NO reduces proliferation of EL4 cells *in vitro[21]*, and thereby provides a possible mechanism for the growth inhibition included in our model. Note that we incorporated a direct effect of IFNγ on tumor proliferation rather than explicitly including this potential cascade of events, because detailed quantitative measurements on these mechanisms are currently lacking.

Although the antiproliferative effect of IFNγ may be an important contributor to tumor control, IFNγ may have had other effects which we did not take into account. First, although we were able to explain regression without a substantial cytotoxic effect of IFNγ, we cannot exclude that possibility. Since such an effect does not act specifically towards tumor cells presenting cognate antigen it may be an important mechanism to control antigen loss variants, which might otherwise allow tumors to recur. Second, IFNγ may induce immuno-tolerance leading to decreased CTL effector function[46]. Third, it has been speculated that IFNγ aids in control of tumors by recruitment of innate effector cells[24], or destruction of tumor vasculature[45]. Our model included neither of these effects because they were not apparent in the experiments we based our model on. However, it is possible that these events happened at a later time, after observations of CTL killing were made. This further underlines that measurements are required throughout the entire course of tumor rejection, in order to gain a full understanding of the sequence of events that occurs.

Apart from the role that IFNγ may play in tumor control, our modeling has also highlighted a potential explanation for temporal variation in measured killing rates of CTLs. Tumor cells may be able to endure multiple attacks from CTLs before apoptosis is triggered[19,44], When we implemented such variability in our model, we indeed found an increase in killing rate over the course of tumor regression. This dependence of killing rate upon measurement time is in agreement with our previous modelling work[36] on T cell-target cell interactions.

A criticism of our approach could be that our simulations do not capture all the myriad complex interactions within the tumor microenvironment. Indeed, our models are a highly idealised representation of reality, since they contain only the mechanisms we explicitly chose to include. This would likely be a problem if using the model as a fully predictive tool for other settings, since the model predictions will not be valid in tumors where unincluded mechanisms are important. However, when applying the model as a diagnostic tool (as we have here), model simplicity is a major advantage. This approach allowed us to quantitatively test whether observations made at the cellular level could explain emergent behaviour of the tumor as a whole, without the interference of confounding variables.

Our work highlights the need for further investigation of indirect effects mediated by CTLs in an anti-tumor immune response. Although many mechanisms utilised by CTLs to control tumors have been identified, quantitative measurements detailing their contribution to regression are scarce. Such quantitative understanding would enable a more sophisticated and systems based understanding of the interplay of various mechanisms in tumor regression following immunotherapy - and likely enable better targeted interventions. Future studies should therefore aim to characterise the potential contribution of various mechanisms to tumor regression. Computational models that integrate *in vitro* and *in vivo* experiments, such as those developed here and as developed by others[47–49], can be a valuable tool to aid in this process.

Acknowledgements

We would like to thank Beatrice Bréart and Philippe Bousso for providing their previously published data and for useful feedback on our modeling of their data. This work is supported by a Vidi grant from the Netherlands Organisation for Scientific Research (NWO; grant 864.12.013 to J.B.B.).

References

1. Jardim DL, de Melo Gagliato D, Giles FJ, Kurzrock R. Analysis of Drug Development Paradigms for Immune Checkpoint Inhibitors. Clin Cancer Res. 2018;24: 1785–1794.

2. Yip A, Webster RM. The market for chimeric antigen receptor T cell therapies. Nat Rev Drug Discov. 2018;17: 161–162.

3. Besser MJ, Shapira-Frommer R, Treves AJ, Zippel D, Itzhaki O, Hershkovitz L, et al. Clinical responses in a phase II study using adoptive transfer of short-term cultured tumor infiltration lymphocytes in metastatic melanoma patients. Clin Cancer Res. 2010;16: 2646–2655.

4. Rosenberg SA, Yang JC, Sherry RM, Kammula US, Hughes MS, Phan GQ, et al. Durable complete responses in heavily pretreated patients with metastatic melanoma using T-cell transfer immunotherapy. Clin Cancer Res. 2011;17: 4550–4557.

5. Chandran SS, Somerville RPT, Yang JC, Sherry RM, Klebanoff CA, Goff SL, et al. Treatment of metastatic uveal melanoma with adoptive transfer of tumour-infiltrating lymphocytes: a single-centre, two-stage, single-arm, phase 2 study. Lancet Oncol. 2017;18: 792–802.

6. Feng K, Guo Y, Dai H, Wang Y, Li X, Jia H, et al. Chimeric antigen receptor-modified T cells for the immunotherapy of patients with EGFR-expressing advanced relapsed/refractory non-small cell lung cancer. Sci China Life Sci. 2016;59: 468–479.

7. Louis CU, Savoldo B, Dotti G, Pule M, Yvon E, Myers GD, et al. Antitumor activity and long-term fate of chimeric antigen receptor-positive T cells in patients with neuroblastoma. Blood. 2011;118: 6050–6056.

8. Ahmed N, Brawley VS, Hegde M, Robertson C, Ghazi A, Gerken C, et al. Human Epidermal Growth Factor Receptor 2 (HER2) -Specific Chimeric Antigen Receptor-Modified T Cells for the Immunotherapy of HER2-Positive Sarcoma. J Clin Oncol. 2015;33: 1688–1696.

9. Larkin J, Chiarion-Sileni V, Gonzalez R, Grob JJ, Cowey CL, Lao CD, et al. Combined Nivolumab and Ipilimumab or Monotherapy in Untreated Melanoma. N Engl J Med. 2015;373: 23–34.

10. Swart M, Verbrugge I, Beltman JB. Combination Approaches with Immune-Checkpoint Blockade in Cancer Therapy. Front Oncol. 2016;6: 233.

11. Pfirschke C, Engblom C, Rickelt S, Cortez-Retamozo V, Garris C, Pucci F, et al. Immunogenic Chemotherapy Sensitizes Tumors to Checkpoint Blockade Therapy. Immunity. 2016;44: 343–354.

12. Weichselbaum RR, Liang H, Deng L, Fu Y-X. Radiotherapy and immunotherapy: a beneficial liaison? Nat Rev Clin Oncol. 2017;14: 365–379.

13. Isaaz S, Baetz K, Olsen K, Podack E, Griffiths GM. Serial killing by cytotoxic T lymphocytes: T cell receptor triggers degranulation, re-filling of the lytic granules and secretion of lytic proteins via a non-granule pathway. Eur J Immunol. 1995;25: 1071–1079.

14. Wiedemann A, Depoil D, Faroudi M, Valitutti S. Cytotoxic T lymphocytes kill multiple targets simultaneously via spatiotemporal uncoupling of lytic and stimulatory synapses. Proc Natl Acad Sci U S A. 2006;103: 10985–10990.

15. Kägi D, Ledermann B, Bürki K, Seiler P, Odermatt B, Olsen KJ, et al. Cytotoxicity mediated by T cells and natural killer cells is greatly impaired in perforin-deficient mice. Nature. 1994;369: 31–37.

16. Smyth MJ, Kershaw MH, Darcy PK, Trapani JA. Adoptive transfer: the role of perforin in mouse cytotoxic T lymphocyte rejection of human tumor xenografts in vivo. Xenotransplantation. 1998;5: 146–153.

17. Caldwell SA, Ryan MH, McDuffie E, Abrams SI. The Fas/Fas ligand pathway is important for optimal tumor regression in a mouse model of CTL adoptive immunotherapy of experimental CMS4 lung metastases. J Immunol. 2003;171: 2402–2412.

18. Breart B, Lemaître F, Celli S, Bousso P. Two-photon imaging of intratumoral CD8+ T cell cytotoxic activity during adoptive T cell therapy in mice. J Clin Invest. 2008;118: 1390–1397.

19. Halle S, Keyser KA, Stahl FR, Busche A, Marquardt A, Zheng X, et al. In Vivo Killing Capacity of Cytotoxic T Cells Is Limited and Involves Dynamic Interactions and T Cell Cooperativity. Immunity. 2016;44: 233–245.

20. Barth RJ Jr, Mulé JJ, Spiess PJ, Rosenberg SA. Interferon gamma and tumor necrosis factor have a role in tumor regressions mediated by murine CD8+ tumor-infiltrating lymphocytes. J Exp Med. 1991;173: 647–658.

21. Hollenbaugh JA, Dutton RW. IFN-γ Regulates Donor CD8 T Cell Expansion, Migration, and Leads to Apoptosis of Cells of a Solid Tumor. The Journal of Immunology. 2006;177: 3004–3011.

22. Matsushita H, Hosoi A, Ueha S, Abe J, Fujieda N, Tomura M, et al. Cytotoxic T lymphocytes block tumor growth both by lytic activity and IFNγ-dependent cell-cycle arrest. Cancer Immunol Res. 2015;3: 26–36.

23. Selleck WA, Canfield SE, Hassen WA, Meseck M, Kuzmin AI, Eisensmith RC, et al. IFN-gamma sensitization of prostate cancer cells to Fas-mediated death: a gene therapy approach. Mol Ther. 2003;7: 185–192.

24. Nagoshi M, Sadanaga N, Joo HG, Goedegebuure PS, Eberlein TJ. Tumor-specific cytokine release by donor T cells induces an effective host anti-tumor response through recruitment of host naive antigen presenting cells. Int J Cancer. 1999;80: 308–314.

25. Briesemeister D, Sommermeyer D, Loddenkemper C, Loew R, Uckert W, Blankenstein T, et al. Tumor rejection by local interferon gamma induction in established tumors is associated with blood vessel destruction and necrosis. Int J Cancer. 2011;128: 371–378.

26. Nguyen HH, Kim T, Song SY, Park S, Cho HH, Jung S-H, et al. Naïve CD8(+) T cell derived tumor-specific cytotoxic effectors as a potential remedy for overcoming TGF-β immunosuppression in the tumor microenvironment. Sci Rep. 2016;6: 28208.

27. Mikucki ME, Fisher DT, Matsuzaki J, Skitzki JJ, Gaulin NB, Muhitch JB, et al. Non-redundant requirement for CXCR3 signalling during tumoricidal T-cell trafficking across tumour vascular checkpoints. Nat Commun. 2015;6: 7458.

28. Yao Y, Chen S, Cao M, Fan X, Yang T, Huang Y, et al. Antigen-specific CD8+ T cell feedback activates NLRP3 inflammasome in antigen-presenting cells through perforin. Nat Commun. 2017;8: 15402.

29. Boissonnas A, Fetler L, Zeelenberg IS, Hugues S, Amigorena S. In vivo imaging of cytotoxic T cell infiltration and elimination of a solid tumor. J Exp Med. 2007;204: 345–356.

30. Hollenbaugh JA, Reome J, Dobrzanski M, Dutton RW. The rate of the CD8-dependent initial reduction in tumor volume is not limited by contact-dependent perforin, Fas ligand, or TNF-mediated cytolysis. J Immunol. 2004;173: 1738–1743.

31. Steinert EM, Schenkel JM, Fraser KA, Beura LK, Manlove LS, Igyártó BZ, et al. Quantifying Memory CD8 T Cells Reveals Regionalization of Immunosurveillance. Cell. 2015;161: 737–749.

32. Parnaik R, Raff MC, Scholes J. Differences between the clearance of apoptotic cells by professional and non-professional phagocytes. Curr Biol. 2000;10: 857–860.

33. Hirano K, Hosoi A, Matsushita H, Iino T, Ueha S, Matsushima K, et al. The nitric oxide radical scavenger carboxy-PTIO reduces the immunosuppressive activity of myeloid-derived suppressor cells and potentiates the antitumor activity of adoptive cytotoxic T lymphocyte immunotherapy. Oncoimmunology. 2015;4: e1019195.

34. Pauken KE, Wherry EJ. Overcoming T cell exhaustion in infection and cancer. Trends Immunol. 2015;36: 265–276.

35. Gadhamsetty S, Marée AFM, Beltman JB, de Boer RJ. A general functional response of cytotoxic T lymphocyte-mediated killing of target cells. Biophys J. 2014;106: 1780–1791.

36. Gadhamsetty S, Marée AFM, Beltman JB, de Boer RJ. A Sigmoid Functional Response Emerges When Cytotoxic T Lymphocytes Start Killing Fresh Target Cells. Biophys J. 2017;112: 1221–1235.

37. Waclaw B, Bozic I, Pittman ME, Hruban RH, Vogelstein B, Nowak MA. A spatial model predicts that dispersal and cell turnover limit intratumour heterogeneity. Nature. 2015;525: 261–264.

38. Beltman JB, Marée AFM, Lynch JN, Miller MJ, de Boer RJ. Lymph node topology dictates T cell migration behavior. J Exp Med. 2007;204: 771–780.

39. Ariotti S, Beltman JB, Chodaczek G, Hoekstra ME, van Beek AE, Gomez-Eerland R, et al. Tissue-resident memory CD8+ T cells continuously patrol skin epithelia to quickly recognize local antigen. Proc Natl Acad Sci U S A. 2012;109: 19739–19744.

40. Halle S, Halle O, Förster R. Mechanisms and Dynamics of T Cell-Mediated Cytotoxicity In Vivo. Trends Immunol. 2017;38: 432–443.

41. Matsushita H, Hosoi A, Ueha S, Abe J, Fujieda N. Cytotoxic T lymphocytes block tumor growth both by lytic activity and IFNγ-dependent cell-cycle arrest. Cancer Immunol. Res. 3, 26–36. doi: 10.1158/2326 …. 2015.

42. Blohm U, Potthoff D, van der Kogel AJ, Pircher H. Solid tumors “melt” from the inside after successful CD8 T cell attack. Eur J Immunol. 2006;36: 468–477.

43. Thomas DA, Massagué J. TGF-beta directly targets cytotoxic T cell functions during tumor evasion of immune surveillance. Cancer Cell. 2005;8: 369–380.

44. Caramalho I, Faroudi M, Padovan E, Müller S, Valitutti S. Visualizing CTL/melanoma cell interactions: multiple hits must be delivered for tumour cell annihilation. J Cell Mol Med. 2009;13: 3834–3846.

45. Schietinger A, Arina A, Liu RB, Wells S, Huang J, Engels B, et al. Longitudinal confocal microscopy imaging of solid tumor destruction following adoptive T cell transfer. Oncoimmunology. 2013;2: e26677.

46. Benci JL, Xu B, Qiu Y, Wu TJ, Dada H, Twyman-Saint Victor C, et al. Tumor Interferon Signaling Regulates a Multigenic Resistance Program to Immune Checkpoint Blockade. Cell. 2016;167: 1540–1554.e12.

47. Gong C, Milberg O, Wang B, Vicini P, Narwal R, Roskos L, et al. A computational multiscale agent-based model for simulating spatio-temporal tumour immune response to PD1 and PDL1 inhibition. J R Soc Interface. 2017;14. doi:10.1098/rsif.2017.0320

48. Byrne HM. Dissecting cancer through mathematics: from the cell to the animal model. Nat Rev Cancer. 2010;10: 221–230.

49. Kather JN, Poleszczuk J, Suarez-Carmona M, Krisam J, Charoentong P, Valous NA, et al. In Silico Modeling of Immunotherapy and Stroma-Targeting Therapies in Human Colorectal Cancer. Cancer Res. 2017;77: 6442–6452.

Table 1: Overview of parameters used in models, what they represent, and their default value. Parameters apply to ABM and ODE model unless indicated otherwise. Parameter values are based on data in Breart *et al.[18]* unless indicated otherwise.

Parameter	**Description**	**Default value**
T0	Number of tumor cells at time 0	1450 (ODE) 180 (ABM)
E0	Number of CTLs at time 0	0
D0	Number of killed tumor cells at time 0	0
k	CTL killing rate	4 kills CTL^{-1} day^{-1}
g	Tumor growth rate	0.86 day^{-1} (ODE) 1.97 day^{-1} (ABM)
d[a]	Disappearance rate of killed tumor cells	2 day^{-1}
p_{arr}	Probability of conjugate formation	1 (ABM)
n_{hit}[b]	Number of hits before tumor cell apoptosis	1 (ABM)
p_{det}	Probability of conjugate splitting	0 (ABM)
p_{disp}	Probability of tumor cell dispersal	0.03 (ABM)
R_i	Initial tumor radius	120µm (ABM)

[a] based on Parnaik *et al.[32]* ; [b] based on Halle *et al.[19]*

Supplementary Data

Video S1. Growth of ABM tumour from day 0 to day 5. EG7 cells that have no available space to divide are indicated in green (others in yellow).

Video S2. CTLs (red) producing IFNγ (purple), which prevents proliferation of EG7 cells (yellow). Video shows day 8, where almost all cells in the tumour centre are affected by IFNγ, but isolated peripheral pockets are escaping.

Video S3. CTLs (red) producing IFNγ (purple) when conjugated with EG7 cells (yellow) but not when conjugated with EL4 cells (blue), in mixed tumours on day 8. IFNγ prevents both tumour cell types from dividing. Note that CTLs congregate in EG7 patches and many EL4 cells remain unaffected.

Supplementary Methods. Additional details of our modeling approach with respect to the killing term employed in the ODE model and IFNγ production and diffusion in the ABM.

Supplementary Methods and Videos S1-S3 are available online (*https://doi.org/10.1158/0008-5472.CAN-18-3147*).